Robert HIERGEIST[1], Klaus WAGNER[1], Gunnar ROSS[1]

Magnet-Physik Dr. Steingroever GmbH, Cologne, Germany (1)

Characterization of Soft Magnetic Materials in AC Magnetic Fields by Digital Methods

Abstract. For the characterization of soft magnetic materials in AC magnetic fields, digital methods are commonly used nowadays. Magnet-Physik offers a family of computer controlled BH-loop tracers. These allow the automated measurement of AC hysteresis loops under various conditions. For instance, an automated separation of the total loss per cycle of the hysteresis loops in dependence of the frequency into hysteretic loss, eddy current loss and anomalous loss (excess loss) is implemented within the software. Furthermore, an automated determination of the total power loss in dependence of H_{max} or B_{max} can be achieved.

Streszczenie. Firma Magnet Physik oferuje rodzinę komputerowo sterowanych testerów pętli histerezy. Umożliwiają one automatyczne badanie pętli histeezy w różnych warunkach. Na przykład możliwa jest automatyczny rozdział strat w unkcji częstotliwości. Ponadto możliwe jest określanie strat w zależności od wartości indukcji inatężenia pola magnetycznego. Badania miękkich materiałów magnetycznych przy prądzie przemiennym metodami cyfrowymi

Keywords: Magnetic core loss, loss separation, Rayleigh loss behavior.
Słowa kluczowe: straty w materiałach magnetycznych, rozdział strat.

Introduction

BH-loop tracers are widely used instruments to measure the AC magnetic properties of soft magnetic specimens. With this class of instruments it is possible to determine characteristic quantities like the remanence B_r, the coercivity H_c, the permeability and the magnetic core loss. For commercial available BH-loop tracers, digital methods are state of the art, eliminating time consuming manual evaluations of the data and allowing a higher throughput of specimens. In addition the usage of digital methods significantly increases the precision of the measurements for instance by averaging the measured data over multiple cycles. In this paper we describe how digital methods are used to determine especially the core loss in dependence of the measurement frequency f (at fixed field amplitude H_{max} or flux density amplitude B_{max}) or in dependence on H_{max} or B_{max} (at fixed measurement frequency f) and the consequences that follow thereof for the materials scientist using these instruments.

Technical Considerations

All measurements with BH-loop tracers working with AC magnetic fields are based on the transformer principle: a primary (magnetizing) winding with N_1 turns around the specimen (e.g. a ring specimen or an Epstein frame specimen) is exerting a magnetic field H into a core made of soft magnetic material. The field is generated by a current I supplied from a power amplifier which is controlled by a programmable signal generator. See fig. 1 (cf. ref. [1], p. 55). In order to estimate the number of turns of the primary winding on a soft magnetic ring core the equation

$$(1) \qquad N_1 \approx \frac{H_{max} \cdot l_m}{I}$$

can be used, where l_m is the length of the magnetic path and H_{max} is the desired maximum magnetic field amplitude over the period of one oscillation cycle. For the case of a thin ring specimen (D/d < 1.4) we can use the formula (see ref. [2], equ. (3))

$$(2.a) \qquad l_m = \pi \cdot \frac{D+d}{2}$$

to determine the length of the magnetic path. Here D is the outer diameter and d is the inner diameter of the ring specimen. For the case of a thick ring specimen (D/d > 1.4) the formula (cf. ref. [1], equ. (5.4))

$$(2.b) \qquad l_m = \pi \cdot \frac{D-d}{\ln(D/d)}$$

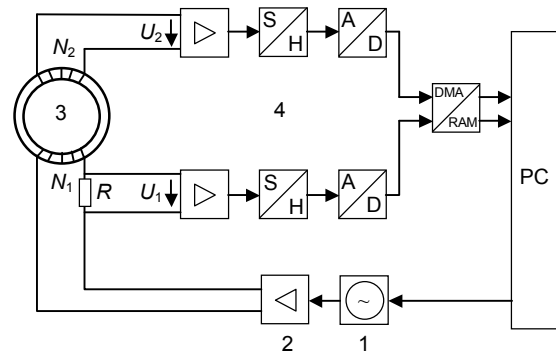should be used. Note that in the limit of a thin ring the results of equ. (2.a) and equ. (2.b) are identical.

Fig.1. Operating principle of the REMACOMP® C BH-loop tracers: 1 programmable signal generator, 2 power amplifier, 3 specimen with a primary winding of N_1 turns and a secondary winding of N_2 turns, 4 data acquisition system: digital sampling system with preamplifiers and analog/digital converters.

For a laminated ring specimen made of non-oriented electrical steel, the desired maximum magnetic field amplitude H_{max} is often in the order of 10 kA/m (cf. the standard EN 10106 [3] and table 1 therein and ref. [4]).

In the case of the Magnet-Physik REMACOMP® C - 200 loop tracer, for example, the current amplitude delivered by the power amplifier (which has to be inserted as I into equ. (1) in order to determine N_1) is at maximum 12 A at a maximum voltage amplitude of 36 V, which cannot be exceeded. Otherwise a clipping of the power amplifier would occur. This would cause a significant distortion of the amplifier signal, which should be avoided.

In order to determine the actual magnetic field amplitude during the oscillation cycle in REMACOMP® loop tracers the current I flowing through the primary winding is measured using a precision shunt resistor R with negligible inductance (cf. fig. 1). (The inductance of the shunt is lower than 10 nH. Therefore, for a frequency of 10 kHz – the maximum

measurement frequency in this paper – we get for $\omega \cdot L$ a value lower than $6.3 \cdot 10^{-4} \cdot \Omega$. The resistance of the shunt depends on the REMACOMP® model. It spreads from 100 mΩ up to 1 Ω. Therefore, even in the worst case scenario of a resistance of only 100 mΩ and a frequency of 10 kHz we obtain a $\omega \cdot L / R$ ratio smaller than $6.3 \cdot 10^{-3}$, which shows that the inductance of the shunt is negligible.)

The secondary winding N_2, which is wound around the specimen as well, is used to measure the induced voltage $U_2(t)$ according to the induction law

$$(3) \qquad U_2(t) = -N_2 \cdot A \cdot \frac{dB}{dt}$$

Here A is the cross-sectional area of the magnetic core and dB/dt the derivation of the flux density B versus time. The secondary winding should be wound around the magnetic core at first. This guarantees a closer distance of the windings to the core and therefore a lower contribution of air flux to the induced voltage. According to the standard IEC 60404-6 (see ref. [2], paragraph 5.2.1 and appendix B), the induced voltage signal measured on the secondary winding N_2 shall be sinusoidal versus time

$$(4) \qquad U_2(t) = U_{2\max} \cdot \sin 2\pi f t \quad .$$

Here $U_{2\max}$ is the amplitude of the induced voltage signal $U_2(t)$. As a consequence of the equs. (3) and (4) this can be accomplished by a cosine type behavior of the induced magnetic flux density across the sample.

$$(5) \qquad B(t) = B_{\max} \cdot \cos 2\pi f t \quad .$$

$B_{\max}$ denotes the magnetic flux density amplitude intended to be used in these measurements. By inserting equs. (4) and (5) into equ. (3) we get for the maximum number of turns of the secondary winding the following estimation

$$(6) \qquad N_2 \leq \frac{U_{2\max}}{A \cdot B_{\max} \cdot 2\pi f} \quad .$$

For $U_{2\max}$ we have to choose a value that must be smaller than the maximum voltage amplitude that can be handled by the input of the BH-loop tracer. (In the case of Magnet-Physik REMACOMP® loop tracers $U_{2\max}$ should be preferably in a range of 0.5 V to 10 V. Thereby the induced voltage signal is smaller than the maximum sustainable input voltage amplitude of 42 V, which must not be exceeded.)

Since the U_2 inputs of digital BH-loop tracers (cf. fig. 1) have a high input resistance, no significant current is flowing though the secondary winding and comparatively thin wires (wire diameter in the order of 0.35 mm) can be used to make the secondary winding.
In contrast, for the primary winding a wire with significantly thicker diameter (wire diameters starting from 0.5 mm) should be chosen.
As a consequence of the behavior described by equ. (4), the so called form factor F_U of the voltage signal, which is the quotient of the root mean square and the average rectified voltages

$$(7) \qquad F_U = \frac{U_{2\mathrm{rms}}}{U_{2\mathrm{avr}}} = \frac{\sqrt{\dfrac{1}{T} \displaystyle\int_{t_0}^{t_0+T} U_2^2(t)\,dt}}{\dfrac{1}{T} \displaystyle\int_{t_0}^{t_0+T} \left| U_2(t) \right|\,dt}$$

should be

$$(8) \qquad F_U = \frac{\pi}{2 \cdot \sqrt{2}} \approx 1.1107 \quad .$$

Deviations of F_U from this value indicate a deviation of $U_2(t)$ from a sinusoidal behavior. Figure 2 shows results of a hysteresis loop measurement of an Epstein-specimen. (For details concerning Epstein measurements see [5-8].) In the lower left corner of this picture, the form factors not only of U_2 (here indicated as u[V]) but as well of H and B (F_U, F_H, and F_B) are shown. Note that the form factors for U and B are both 1.110 and therefore very close to the form factor of a sinusoidal signal of 1.1107. However, also non-sinusoidal signals can have form factors close to 1.1107. Therefore it is important to keep attention on the $U_2(t)$ and $B(t)$ waveform shapes during the measurements, in order to make sure that both signals are actually sinusoidal. Alternatively, instead of the $U_2(t)$ and $B(t)$ plots, the maximal deviations from sinusoidal curves of the $U_2(t)$ and $B(t)$ signals can be observed.

Experimental Results
1. Loss Separation
The software included with the different REMACOMP® BH-loop tracers offers the possibility to automatically measure hysteresis loops and to calculate the total core power loss density P in Watt/m^3. This is done by integrating the area inside the BH-loops and multiplying this quantity by the frequency f. From these data, the weight specific total power loss P_S can be obtained by dividing P by the density of the material. Furthermore, by dividing this quantity by the frequency we get the total loss per cycle in Joule/kg. An automated separation of the total core loss per cycle into hysteretic loss W_h (which is independent of the frequency), eddy current loss $W_e = C_e \cdot f$ and anomalous loss W_a (also called excess loss) with $W_a = C_a \cdot \sqrt{f}$ according to.

$$(9) \qquad P_S(f)/f = W_h + W_e + W_a = C_h + C_e \cdot f + C_a \cdot \sqrt{f}$$

is implemented within the software. For details concerning the different loss contributions see [9-11]. An explicit calculation of the coefficients C_e and C_a in dependence on - for instance - the conductivity σ of the material is given in ref. [9]. Since the conductivity of the specimens is in general unknown, a fitting algorithm is used in the REMACOMP® software to determine the different loss contributions in equ. (9).
Examples of this separation of the loss per cycle in dependence on the frequency are shown in fig. 3 (a)-(d) for four different specimens.
Figure 3 (a) and (b) show loss data of measurements made with a REMACOMP® C - 1200 loop tracer (output ratings of this instrument are a maximum output current amplitude of 30 A and a maximum output voltage amplitude of 150 V) using a standard 25 cm Epstein frame for a non-oriented (NO) and a grain-oriented (GO) electrical steel specimen, respectively. Note the very low hysteretic loss W_h in the case of the GO sample in comparison to the NO sample, despite of the fact that in the latter case a higher $B_{\max}$ was chosen.
Figure 3 (c) and (d) show data of ring cores obtained from measurements with a REMACOMP® C - 200 up to frequencies of 10 kHz. The specimens are ring cores made of a nanocrystalline alloy and of a soft magnetic ferrite, respectively. Note here the very low loss in in both cases (c) and (d) and the very low W_e and W_a values in (d) due to the very high resistivity of the soft magnetic ferrite. The

REMACOMP®-controlling software allows either a setting of the maximum field amplitude (i.e. a setting of $H_{\max}$) or a setting of the maximum flux density amplitude (i.e. a setting of $B_{\max}$) of the hysteresis loop to be measured. In the case of fig. 3 (a, b, d) $B_{\max}$ was set for the measurement of these hysteresis loops. In contrast in fig. 3 (c) a maximum field amplitude (i.e. $H_{\max}$) was set for theses loop measurements. In all those four cases fig. 3 shows a good agreement of the sum of the separated losses and the experimental data points of the total loss per cycle in dependence on the frequency.
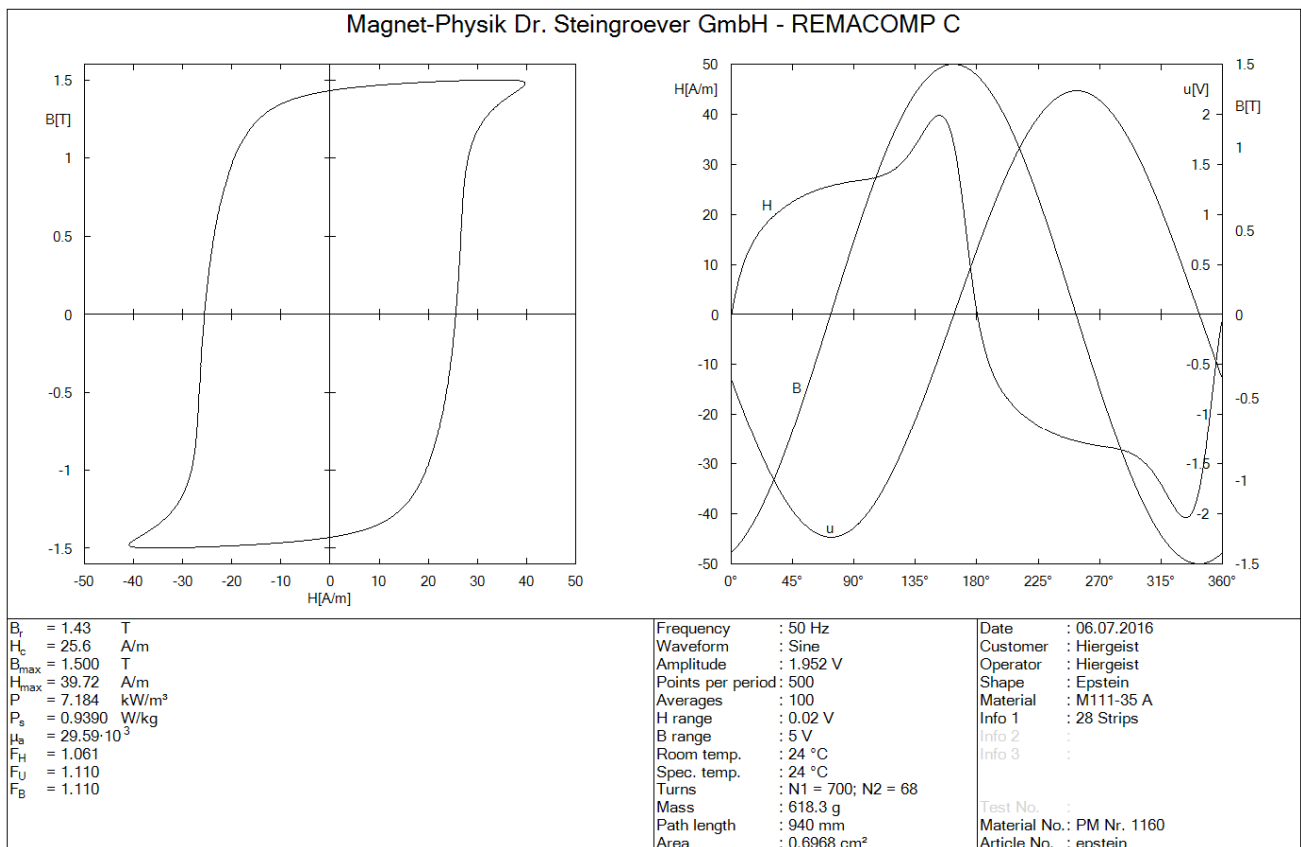

Fig.2. Screen shot of the REMACOMP® BH-loop tracer software. A typical hysteresis loop of a grain-oriented SiFe Epstein specimen (M111-35A) is shown here in the left diagram. On the right hand side a combined diagram for H, U_2 (here labeled as u[V]) and B in dependence of the phase angle $(2\pi ft)$ is depicted. Note the nearly perfect sinusoidal behavior of U_2 and B. This is due to the digital feedback of the U_2 signal in the software. As a consequence of this feedback, the H-signal is not sinusoidal and the form factor $F_H = 1.061$ shows a significant deviation from the value given in equ. (8) for a sinusoidal behavior.

2. Rayleigh Loops: Loss in Low Magnetic Fields

The software included with the REMACOMP® loop tracers does not only allow an automated loss separation as shown above, but also an automated measurement of a set of hysteresis loops with increasing excitation amplitudes at a fixed frequency (i.e. minor loops).

For such a set of minor loops, the weight specific total power loss P_S in Watts per kg is plotted in fig. 4 as a function of the minor loop field amplitude $H_{\max}$ for a soft magnetic ferrite ring core specimen measured at a frequency of 50 Hz. P_S is increasing with $H_{\max}^3$ for small values of $H_{\max}$ (solid line). This increase of P_S with $H_{\max}^3$ is characteristic of the so called Rayleigh loops, usually found in DC measurements for minor loops at low magnetic fields [12-15].

In soft magnetic ferrites, especially at 50 Hz, the hysteretic loss is dominating and dynamic loss (eddy current loss and anomalous loss) is negligible due the high resistivity of this material. The dominance of the hysteretic loss at 50 Hz can be seen in fig. 3(d). Therefore, in fact data of the hysteretic loss are plotted in Fig. 4 in dependence of the minor loop field amplitude $H_{\max}$ and the typical Rayleigh behavior $P_S \propto H_{\max}^3$ could be observed for low field amplitudes.

3. Power Law Behavior of Total Loss in Dependence on B_{max}

Data of the total weight specific power loss P_S in dependence on the minor loop flux density amplitude $B_{\max}$ for several minor loops measured on (a) a non-oriented electrical steel Epstein specimen M330-35 (cf. fig. 3 (a)) and (b) a grain-oriented electrical steel Epstein specimen M111-35A (cf. fig. 3 (b)) are shown in fig. 5 for a measurement frequency of 50 Hz in a log-log plot.

As it can be observed in this plot, there is a very good agreement between the data points and the power law of the form $P_S = \text{const } B_{\max}^p$, except for very high values of the flux density amplitude $B_{\max}$, as indicated by the two straight fitting lines in fig. 5. As expected, the data show a much higher specific power loss for the non-oriented electrical steel in contrast to the grain-oriented steel specimen. By fitting the power law $P_S = \text{const } B_{\max}^p$ to the experimental data, we find a power $p = 1.73$ in the case of the non-oriented steel and $p = 1.89$ in the case of the grain-oriented steel, respectively.
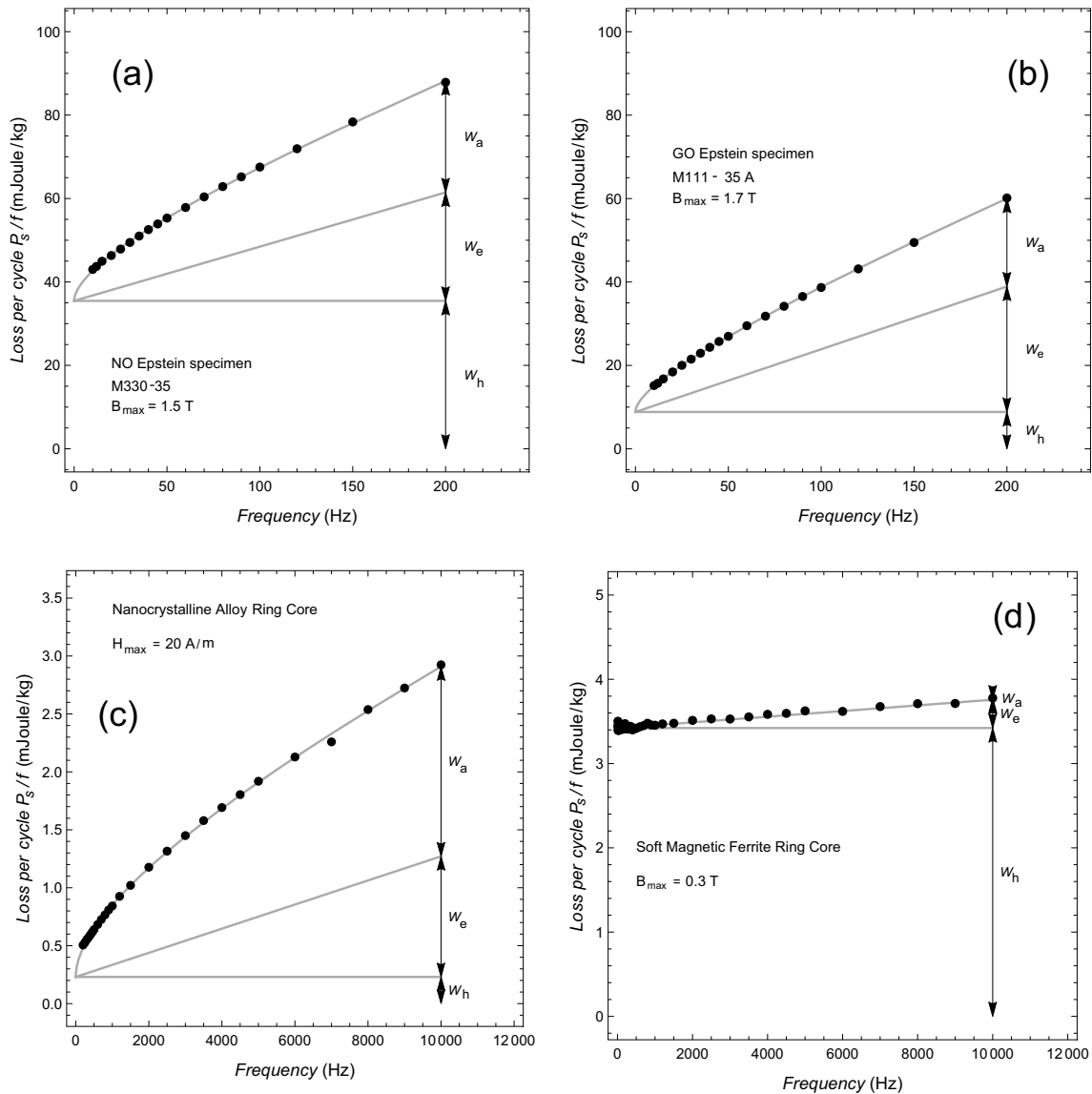
Fig.3. Examples of the separation of loss per cycle in dependence on the frequency for four different specimens of soft magnetic material.

A similar power law behavior but for the hysteretic loss contribution was found by Steinmetz [16], who observed a rather accurate agreement with $W_h \propto B_{max}^{1.6}$ [17]

Discussion

In the last paragraph we showed experimental results of measurements on soft ferromagnetic materials in AC magnetic fields with computer controlled BH-loop tracers. We demonstrated the abilities to separate the frequency dependent loss contributions for four different specimens of soft magnetic material.

A typical Rayleigh loss behavior was found in the case of hysteretic loss in dependence of the magnetic field amplitude for a soft magnetic ferrite ring core specimen for low magnetic field amplitudes.

Finally, a phenomenological power law behavior of the total power loss in dependence of the flux density amplitude of minor loops was found for a non-oriented and a grain-oriented electrical steel specimen.
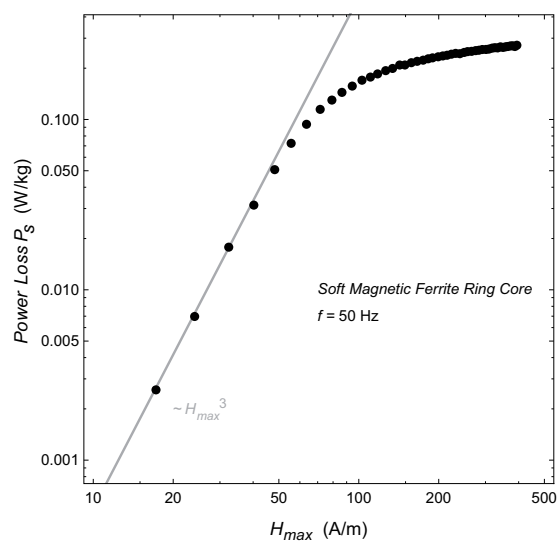

Fig.4. Log-log plot of the total weight specific power loss P_S in dependence on the field amplitude H_{max} of a soft magnetic ferrite ring core specimen. Note the increase of P_S with H_{max}^3 for small values of H_{max} (solid line).
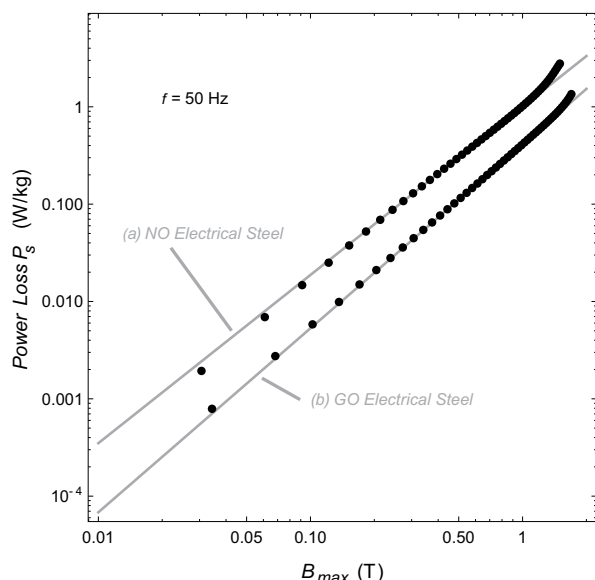
Fig.5. Log-log plot of the total weight specific power loss P_S of minor loops in dependence on their flux density amplitude B_{max} of a non-oriented electrical steel Epstein specimen (a) and of a grain-oriented electrical steel Epstein specimen (b). Note the increase of P_S with B_{max}^p in both cases for a broad range of flux density amplitudes indicated by the straight solid lines.

Authors: *dr rer. nat. Robert Hiergeist, Magnet-Physik Dr. Steingroever GmbH, Emil-Hoffmann-Straße 3, 50996 Köln, Germany, E-mail: robert.hiergeist@magnet-physik.de; dr rer. nat. Klaus Wagner, Magnet-Physik Dr. Steingroever GmbH, Emil-Hoffmann-Straße 3, 50996 Köln, Germany, E-mail: klaus.wagner@magnet-physik.de; dr inż. Gunnar Ross, Magnet-Physik Dr. Steingroever GmbH, Emil-Hoffmann-Straße 3, 50996 Köln, Germany, E-mail: gunnar.ross@magnet-physik.de.*

REFERENCES

[1] Steingroever E., Ross G., Magnetic Measuring Techniques, 2008
[2] IEC 60404-6, Magnetic materials-Part 6: Methods of measurements of the magnetic properties of soft metallic and powder materials at frequencies in the range of 20 Hz to 200 kHz by the use of ring specimens , IEC, Geneva, 2003
[3] IEC 60404-1, Magnetic materials, IEC, Geneva, 2008
[4] EN 10106, Cold rolled non-oriented electrical steel sheet and strip delivered in the fully processed state, CEN, Brüssel, 2007, Table 1
[5] IEC 60404-2, Methods of Measurement of the Magnetic Properties of Electrical Strip and Sheet by means of an Epstein Frame, IEC, Geneva, 2009
[6] ASTM A343/A343M, Standard Test Method for Alternating-Current Magnetic Properties of Materials at Power Frequencies Using Wattmeter-Ammeter-Voltmeter Method and 25-cm Epstein Test Frame, Annual Book of ASTM, 03.04 Magnetic Properties, 2012, 38-53
[7] ASTM A889/A889M, Standard Test Method for Alternating-Current Magnetic Properties of Materials at Low Magnetic Flux Density Using the Voltmeter-Ammeter-Wattmeter-Varmeter-Method and 25-cm Epstein Frame, Annual Book of ASTM, 03.04 Magnetic Properties, 2012, 211-215
[8] ASTM A348/A348M, Standard Test Method for Alternating Current Magnetic Properties of Materials Using the Wattmeter-Ammeter-Voltmeter Method, 100 to 10000 Hz and 25-cm Epstein Frame, Annual Book of ASTM, 03.04 Magnetic Properties, 2012, 58-67
[9] Bertotti G., Fiorillo F., Soardo G.P., The Prediction of Power Losses in Soft Magnetic Materials, Journal De Physique C8 S12 49 1988, 1915
[10] Najgebauer M., Models for Prediction of Energy Loss in Soft Magnetic Materials, XII International PhD Workshop OWD 2010, 23-26 October 2010, 477-482
[11] Hilzinger R., Rodewald W., Magnetic Materials, Publicis Publishing, ISBN 978-89578-352-4, 2013, 125
[12] Chikazumi S., Physics of Magnetism, Oxford University Press, 1997, 499
[13] Kneller E., Ferromagnetismus, Springer 1962, 558
[14] Fiorillo F., Measurement and Characterization of Magnetic Materials, Elsevier 2004, 22
[15] Cullity B.C., Graham C.D., Introduction to Magnetic Materials, John Wiley&Sons, 2009, 322
[16] Steinmetz C.P., On the Law of Hysteresis, Trans. Am. Ist. Elec. Engrs. 9, 1892, 3-64
[17] Bozorth R.M., Ferromagnetism, John Wiley & Sons, New Jersey, 2003, 509